Time-Domain Realisations of 2.5-Dimensional Local Sound Field Synthesis

Fiete Winter and Sascha Spors

Institute of Communications Engineering, University of Rostock, R.-Wagner-Str. 31 (H8), D-18119 Rostock, Germany

Email: {fiete.winter, sascha.spors}@uni-rostock.de

1 Introduction

Sound Field Synthesis aims at a physically accurate synthesis of a desired sound field inside an extended listening area. Wave Field Synthesis (WFS) [1] and Near-Field-Compensated Higher Order Ambisonics (NFC-HOA) [2] are well established representatives of these methods. While the theory of Sound Field Synthesis (SFS) assumes a continuous distribution of acoustic sources placed around the listening area to reproduce the desired sound field, a limited number (up to hundreds) of individually driven loudspeakers placed at discrete positions approximates this distribution in practice. The synthesis accuracy is mainly limited by spatial aliasing artefacts due to the finite resolution of this discretisation. Local Sound Field Synthesis (LSFS) increases the accuracy inside a limited target region while stronger artefacts outside are permitted. Several approaches [3–7] for LSFS have been proposed within the past decade. An approach [8] for Local Wave Field Synthesis (LWFS) uses a distribution of focused sources as virtual loudspeakers surrounding the target region. Analogue to conventional SFS these virtual loudspeakers are driven by a suitable SFS technique in order to reproduce the desired sound field. The SFS driven focused sources are synthesised by the real loudspeaker setup. However, the actual real-time implementation of this approach has not been sufficiently tackled. This paper proposes time-domain realisations for the mentioned synthesis method and compares them to conventional WFS with regard to practicability and computational effort. Hereby, dynamic aspects like e.g. moving sound sources and a moving target region are considered.

2 (Local) Sound Field Synthesis

The fundamental task in LSFS is to reproduce a desired (aka. virtual) sound field $S(\mathbf{x},\omega)$ within a defined listening region $\Omega_l \subseteq \Omega$ (cf. Fig. 1). In $2^1/_2$-dimensional (2.5D) scenarios [9, Sec. 2.3], reproduction is restricted to the horizontal plane, i.e. $z = 0$, and Ω_l and Ω are hence two-dimensional areas. For the special case where $\Omega_l = \Omega$, approaches are usually referred to as conventional SFS. A distribution of loudspeakers is positioned along the boundary $\partial\Omega$ as so-called secondary sources. Each secondary source is oriented along the inward pointing boundary normal $\mathbf{n}_0(\mathbf{x}_0)$. The sound field emitted by an individual secondary source is commonly modelled by a monopole point source. It is given by the three-dimensional free field Green's function [10, Eq.(8.41)] $G(\mathbf{x}|\mathbf{x}_0,\omega)$ with $\mathbf{x}_0 \in \partial\Omega$. Each individual secondary source is driven by its respective driving signal $D(\mathbf{x}_0,\omega)$

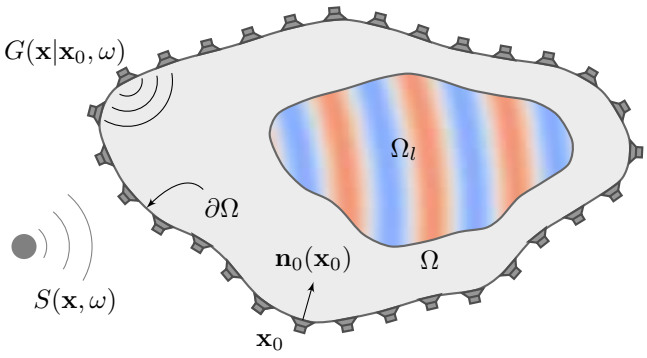

Figure 1: Illustration of (Local) Sound Field Synthesis. The loudspeakers aka. secondary sources are indicated by the loudspeaker symbols.

and the resulting superposition of all secondary sources constitutes the reproduced sound field. The driving signals have to be chosen such that the reproduced and the desired sound field coincide within Ω_l. Mathematically, this is subsumed by

$$S(\mathbf{x},\omega) \overset{!}{=} \oint_{\partial\Omega} D(\mathbf{x}_0,\omega) G(\mathbf{x}|\mathbf{x}_0,\omega)\,\mathrm{d}l(\mathbf{x}_0)\;\forall \mathbf{x} \in \Omega_l\,. \quad (1)$$

A suitably chosen differential line segment for the integration along the boundary $\partial\Omega$ is denoted by $\mathrm{d}l(\mathbf{x}_0)$.

3 Wave Field Synthesis

3.1 Driving Signals

WFS is based on a high-frequency approximation of the Helmholtz Integral Equation (HIE). For 3D scenarios, the driving function is generally given by [11, Eq. (10)]

$$D^{\mathrm{WFS}}(\mathbf{x}_0,\omega) = -2\,a_S(\mathbf{x}_0)\,\left\langle \nabla_{\mathbf{x}_0} S(\mathbf{x}_0,\omega) \middle| \mathbf{n}_0(\mathbf{x}_0) \right\rangle \quad (2)$$

where $\nabla_{\mathbf{x}_0}$ denotes the gradient w.r.t. $\mathbf{x}_0$. The selection criterion $a_S(\mathbf{x}_0)$ activates only the secondary sources, whose normal $\mathbf{n}_0(\mathbf{x}_0)$ points in the direction of propagation of the virtual sound field at $\mathbf{x}_0$. This treatise covers the two propably most often used virtual sound fields in model based sound field synthesis, namely the plane wave and point source. For 2.5D synthesis scenarios, correct synthesis with respect to amplitude is only possible at a pre-defined reference point or on a reference curve. Former will be denoted as $\mathbf{x}_{\mathrm{ref}}$. For a virtual point source located at $\mathbf{x}_{\mathrm{ps}} \notin \Omega$, the WFS driving signal using the reference point reads [12, Eq. (2.137)]

$$\begin{aligned} D^{\mathrm{WFS}}_{\mathrm{ps}}(\mathbf{x}_0,\omega) &= \hat{S}(\omega)\sqrt{\frac{\mathrm{j}\omega}{\mathrm{c}}}\mathrm{e}^{-\mathrm{j}\frac{\omega}{\mathrm{c}}|\mathbf{x}_0-\mathbf{x}_{\mathrm{ps}}|} \\ &\times \frac{1}{\sqrt{2\pi}} \frac{\langle \mathbf{x}_0-\mathbf{x}_{\mathrm{ps}} | \mathbf{n}_0(\mathbf{x}_0)\rangle a_{\mathrm{ps}}(\mathbf{x}_0)\sqrt{|\mathbf{x}_0-\mathbf{x}_{\mathrm{ref}}|}}{|\mathbf{x}_0-\mathbf{x}_{\mathrm{ps}}|^{3/2}\sqrt{|\mathbf{x}_0-\mathbf{x}_{\mathrm{ps}}|+|\mathbf{x}_0-\mathbf{x}_{\mathrm{ref}}|}}\,, \end{aligned} \quad (3)$$

where $a_{\mathrm{ps}}(\mathbf{x}_0)$ denotes the secondary source selection criterion for a point source. The Fourier spectrum of the source signal emitted by the point source is described by $\hat{S}(\omega)$. The corresponding driving signal for a virtual plane wave propagating in the direction of $\mathbf{n}_{\mathrm{pw}}$ is given as [12, Eq. (2.177)]

$$D_{\mathrm{pw}}^{\mathrm{WFS}}(\mathbf{x}_0,\omega) = \hat{S}(\omega)\sqrt{\frac{\mathrm{j}\omega}{\mathrm{c}}}\mathrm{e}^{-\mathrm{j}\frac{\omega}{\mathrm{c}}\langle\mathbf{x}_0|\mathbf{n}_{\mathrm{pw}}\rangle} \times \sqrt{8\pi|\mathbf{x}_0-\mathbf{x}_{\mathrm{ref}}|}\, a_{\mathrm{pw}}(\mathbf{x}_0)\langle\mathbf{n}_{\mathrm{pw}}|\mathbf{n}_0(\mathbf{x}_0)\rangle\,, \tag{4}$$

where $a_{\mathrm{pw}}(\mathbf{x}_0)$ denotes the secondary source selection criterion for a plane wave. Both driving functions exhibit a common structure: i) A geometry independent pre-filter $H_{\mathrm{pre}}(\omega) = \sqrt{\mathrm{j}\omega/\mathrm{c}}$. ii) The exponential term represents a geometry dependent delay operation, whereas the corresponding delay is subsumed under $\tau(\mathbf{x}_0)$. iii) The remaining term is a geometry dependent scalar weighting factor represented by $w(\mathbf{x}_0)$ in the following.

3.2 Time-Domain Realisation

For the implementation, the inverse Fourier transform is applied to the WFS driving functions. Furthermore, a temporal sampling with a sampling period of T_s is applied. The discrete time-domain driving signals can be given in general form as

$$d^{\mathrm{WFS}}[\mathbf{x}_0,n] = w(\mathbf{x}_0)h_{\mathrm{pre}}[n]*_n\hat{s}[n]*_n\delta\left[n-\frac{\tau(\mathbf{x}_0)}{T_s}\right]. \tag{5}$$

Note, that this formula does only cover the driving function for a single virtual source. In practice, the driving signal for different sources is added in order to render the whole virtual scene. The number of virtual sources and loudspeakers are denoted by N_{s} and L, respectively. As illustrated in Fig. 2, the rendering can be implemented in three essential steps: i) As the pre-filter $h_{\mathrm{pre}}[n]$ is geometry independent it can be either directly applied to each source signal $s[n]$ or to each driving signal of loudspeakers. Latter is more efficient, if $L < N_{\mathrm{s}}$. The computational costs for a single pre-filtering operation is denoted by c_{pre}. It depends on several aspects, e.g. its implementation (finite or infinite impulse response) and the number of filter coefficients. ii) The (possibly pre-filtered) source signal is stored in a delayline. A delayline is essentially a signal buffer, from which delayed and weighted versions of the source signal can be requested. The effort for writing a signal into a delayline is subsumed under c_{write}. iii) The costs for a single request from the delay together with the subsequent add-operation is defined as c_{read}. The overall costs for WFS can hence be expressed as

$$c_{\mathrm{I}}^{\mathrm{WFS}}(N_{\mathrm{s}},L) = N_{\mathrm{s}}c_{\mathrm{pre}} + N_{\mathrm{s}}c_{\mathrm{write}} + N_{\mathrm{s}}Lc_{\mathrm{read}}\,, \tag{6a}$$

$$c_{\mathrm{II}}^{\mathrm{WFS}}(N_{\mathrm{s}},L) = N_{\mathrm{s}}c_{\mathrm{write}} + N_{\mathrm{s}}Lc_{\mathrm{read}} + Lc_{\mathrm{pre}}\,, \tag{6b}$$

while I and II cover the pre-filtering options given in Fig. 2. It can be seen that the costs for read-operations scales with LN_{s}, while the write-operations do only scale with N_{s}. It is hence desired to keep c_{read} as low a possible.

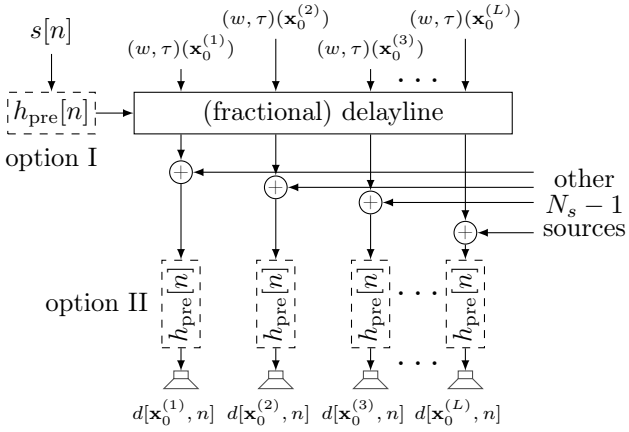

Figure 2: Block-Diagram showing the time-domain realisation of Wave Field Synthesis for one virtual source. Contributions from other virtual source are incorporated via the "+"-operators.

The delays $\tau(\mathbf{x}_0)$ are generally not an integer multiple of the sample period T_s. Furthermore, the change of the scene geometry over time, e.g. moving sound sources, results in time-variant delays. Hence, interpolation has to be applied to the sampled source signal in order to retrieve signal values for inter-sample position. An extensive overview about the realisation of fractional delay interpolation and arbitrary sample rate conversion for WFS is given in [13]. For the macroscopic analysis within this paper, it is sufficient to classify the methods into three categories: i) Rounding the delay to the next integer delay is the simplest variant, which results in relatively low c_{write} and c_{read}. It has been shown in [14, Sec. 7], that this approach it is perceptually sufficient for stationary scenarios reproduced with a circular loudspeaker array (1.5 metre radius, 56 loudspeakers) at a sampling frequency of 44.1 kHz. According to [15, Sec. 3.2], audible artefacts however occur in dynamic scenarios even for slow source movements. ii) The interpolation is done upon request, resulting in a low c_{write} and no additional memory requirements since the source signal stored as is in the delayline. c_{read} is comparably high due to the interpolation. iii) A delay independent preprocessing is an efficient alternative to the prior category. A prominent example is the oversampling of the signal about an integer factor. The oversampled signal is stored in the delayline. Upon request, the delay is rounded to the next integer in the oversampled domain and the delayed signal is downsampled, again. Here, the c_{read} is significantly lower than for the second category, while c_{write} is higher. As a drawback, additional memory is required to store the oversampled signal.

4 Local Wave Field Synthesis

4.1 Driving Signals

Some SFS techniques, such as WFS, allow for the reproduction of so-called focused sources which approximate the sound field of a monopole point source located inside Ω. A set of focused sources is utilized as a virtual

secondary source distribution, which is driven like a real loudspeaker setup. The virtual secondary sources are distributed along $\partial\Omega_l$ (cf. Fig. 1). The loudspeakers' driving function is given as

$$D^{\mathrm{LWFS}}(\mathbf{x}_0,\omega) = \oint_{\partial\Omega_l} D^{\mathrm{WFS}}(\mathbf{x}_{\mathrm{fs}},\omega) D^{\mathrm{WFS}}_{\mathrm{fs}}(\mathbf{x}_0|\mathbf{x}_{\mathrm{fs}},\omega)\,\mathrm{d}l(\mathbf{x}_{\mathrm{fs}})\,, \tag{7}$$

where $D^{\mathrm{WFS}}(\mathbf{x}_{\mathrm{fs}},\omega)$ denotes the WFS driving function applied for each virtual secondary source to reproduce $S(\mathbf{x})$ inside Ω_l. The driving function to reproduce a particular focused source located at $\mathbf{x}_{\mathrm{fs}} \in \partial\Omega_l$ is denoted by $D^{\mathrm{WFS}}_{\mathrm{fs}}(\mathbf{x}_0|\mathbf{x}_{\mathrm{fs}},\omega)$. Latter is given by its 2.5D variant [9, Eq. (A.14)]

$$D^{\mathrm{WFS}}_{\mathrm{fs}}(\mathbf{x}_0|\mathbf{x}_{\mathrm{fs}},\omega) = \sqrt{\frac{-\mathrm{j}\omega}{\mathrm{c}}}\mathrm{e}^{+\mathrm{j}\frac{\omega}{\mathrm{c}}|\mathbf{x}_{\mathrm{fs}}-\mathbf{x}_0|} \times \frac{1}{\sqrt{2\pi}} \frac{\langle \mathbf{x}_{\mathrm{fs}}-\mathbf{x}_0|\mathbf{n}_0(\mathbf{x}_0)\rangle a_{\mathrm{fs}}(\mathbf{x}_0)\sqrt{|\mathbf{x}_{\mathrm{ref}}-\mathbf{x}_0|}}{|\mathbf{x}_{\mathrm{fs}}-\mathbf{x}_0|^{3/2}\sqrt{||\mathbf{x}_{\mathrm{ref}}-\mathbf{x}_0|-|\mathbf{x}_{\mathrm{fs}}-\mathbf{x}_0||}}\,, \tag{8}$$

which has the same structure as described in Sec. 3.1. Due to computational constraints, only a finite number of focused sources is positioned at discrete positions along $\partial\Omega_l$ can be employed. Hence, the integral in (7) is approximated by the sum

$$D^{\mathrm{LWFS}}(\mathbf{x}_0,\omega) = \sum_{\mathbf{x}_{\mathrm{fs}}\in\mathcal{X}_{\mathrm{fs}}} D^{\mathrm{WFS}}(\mathbf{x}_{\mathrm{fs}},\omega) D^{\mathrm{WFS}}_{\mathrm{fs}}(\mathbf{x}_0|\mathbf{x}_{\mathrm{fs}},\omega)\,, \tag{9}$$

with $\mathcal{X}_{\mathrm{fs}}$ being the set of focused sources with the cardinality $N_{\mathrm{fs}} := |\mathcal{X}_{\mathrm{fs}}|$. Due to the common structure of (3), (4), and (8), the LWFS driving function can be expressed as

$$D^{\mathrm{LWFS}}(\mathbf{x}_0,\omega) = |H_{\mathrm{pre}}(\omega)|^2 \sum_{\mathbf{x}_{\mathrm{fs}}\in\mathcal{X}_{\mathrm{fs}}} w(\mathbf{x}_0|\mathbf{x}_{\mathrm{fs}})\,\mathrm{e}^{-\mathrm{j}\omega\tau(\mathbf{x}_0|\mathbf{x}_{\mathrm{fs}})}\,, \tag{10}$$

with $w(\mathbf{x}_0|\mathbf{x}_{\mathrm{fs}})$ and $\tau(\mathbf{x}_0|\mathbf{x}_{\mathrm{fs}})$, again, denoting a geometry dependent weight and delay, respectively.

4.2 Time-Domain Realisation

The discrete time driving signal finally reads

$$d^{\mathrm{LWFS}}[\mathbf{x}_0,n] = \hat{s}[n] *_n \hat{h}_{\mathrm{pre}}[n] *_n \sum_{\mathbf{x}_{\mathrm{fs}}\in\mathcal{X}_{\mathrm{fs}}} w(\mathbf{x}_0|\mathbf{x}_{\mathrm{fs}})\,\delta\left[n - \frac{\tau(\mathbf{x}_0|\mathbf{x}_{\mathrm{fs}})}{T_s}\right]\,. \tag{11}$$

The discretised inverse Fourier transform of the squared pre-filter in (10) is denoted as $\hat{h}_{\mathrm{pre}}[n]$. In the following, two architectures for implementation will be presented:

2-Stage Realisation: As (9) states the combination of two WFS driving functions, the intuitive concept of connecting two (possibly already existing) WFS realisations arises. The concept is illustrated in Fig. 4a: In the first component, the driving signals for the virtual secondary sources are computed. In the second component, these driving signals are used as the source signals for the focused sources which are to be synthesized by the loudspeakers. The corresponding cost function reads

$$c^{\mathrm{LWFS}}_{\mathrm{2Stage}}(N_{\mathrm{s}},N_{\mathrm{fs}},L) = c^{\mathrm{WFS}}(N_{\mathrm{s}},N_{\mathrm{fs}}) + c^{\mathrm{WFS}}(N_{\mathrm{fs}},L)\,, \tag{12}$$

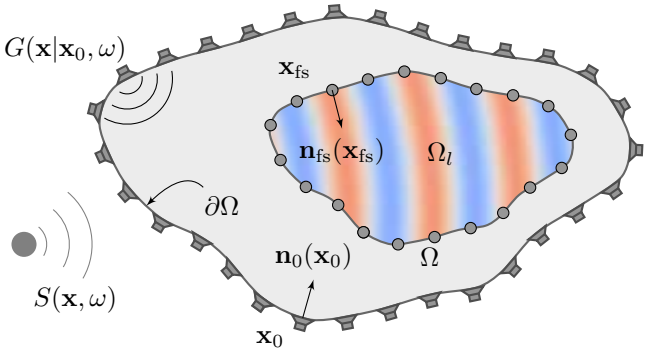

Figure 3: Illustration of Local Wave Field Synthesis. The focused sources are indicated by the bullets shaded in grey.

where c^{WFS} can be either of the options in (6). Using option I in both WFS components results in

$$c^{\mathrm{LWFS}}_{\mathrm{2Stage}}(N_{\mathrm{s}},N_{\mathrm{fs}},L) = (N_{\mathrm{s}}+N_{\mathrm{fs}})c_{\mathrm{pre}} + (N_{\mathrm{s}}+N_{\mathrm{fs}})c_{\mathrm{write}} + N_{\mathrm{fs}}(N_{\mathrm{s}}+L)c_{\mathrm{read}}\,. \tag{13}$$

The strategy can be slightly improved by omitting the pre-filtering in the second stage and applying $\hat{h}_{\mathrm{pre}}[n]$, cf. (11), in the first stage, instead of $h_{\mathrm{pre}}[n]$. The resulting cost function

$$c^{\mathrm{LWFS}}_{\mathrm{2Stage}}(N_{\mathrm{s}},N_{\mathrm{fs}},L) = N_{\mathrm{s}}c_{\mathrm{pre}} + (N_{\mathrm{s}}+N_{\mathrm{fs}})c_{\mathrm{write}} + N_{\mathrm{fs}}(N_{\mathrm{s}}+L)c_{\mathrm{read}} \tag{14}$$

has a reduced effort for the pre-filtering. Similar to the conventional WFS, the scaling factors for the delayline costs are compared: for realistic cases, i.e. $N_{\mathrm{fs}} > 0$, $N_{\mathrm{s}} > 0$, and $L > 0$, the inequality

$$(N_{\mathrm{s}}+N_{\mathrm{fs}}) \leq N_{\mathrm{fs}}(N_{\mathrm{s}}+L) \tag{15}$$

holds. Hence, it is also important for this realisation to prioritise low c_{read}. Compared to the WFS realisation, N_{fs} additional delaylines for the second WFS component are needed to store the driving signals of the focused sources.

Direct Realisation: The direct implementation of (11) is illustrated in Fig. 4b. Compared to the WFS realisation, the number of requests from the delayline additionally scales with a number of focussed sources N_{fs}. The corresponding cost function reads

$$c^{\mathrm{LWFS}}_{\mathrm{direct}}(N_{\mathrm{s}},N_{\mathrm{fs}},L) = N_{\mathrm{s}}c_{\mathrm{pre}} + N_{\mathrm{s}}c_{\mathrm{write}} + N_{\mathrm{fs}}LN_{\mathrm{s}}c_{\mathrm{read}}\,. \tag{16}$$

The question arises, under which conditions the costs in (14) supersede the ones in (16). This is the case, if

$$c_{\mathrm{write}} \geq (LN_{\mathrm{s}} - N_{\mathrm{s}} - L)c_{\mathrm{read}}\,. \tag{17}$$

Since both realisations benefit from a delay independent pre-processing for the delay interpolation which was presented in Sec. 3.2, c_{write} is mainly determined by the required accuracy of the delay interpolation. Although no final statements can be made without knowledge about the actual values of c_{write} and c_{read}, the direct realisation

is likely to be more efficient for high-resolution delay interpolation. Furthermore, it requires only N_s instead of $N_\mathrm{s} + N_\mathrm{fs}$ delaylines. For low-resolution delay interpolation including integer delays, the 2-stage approach should be preferred.

5 Conclusion

This paper presented two practical implementations for LWFS using focused sources as virtual loudspeakers. Their computational costs and memory requirements where compared with each other and with an realisation of WFS on a macroscopic level. In general, the computational cost of the geometry-independent pre-filtering depends on the stage at which it is applied. For the delay interpolation, a delay independent preprocessing reduces computational costs but requires more memory compared to other alternatives. The 2-stage approach for LWFS may employ already existing realisations of WFS, e.g. the SoundScape Renderer [16]. The direct implementation of LWFS may be used, if a high-accuracy delay interpolation is required.
It remains future work to evaluate and compare the run time of realisations in a fair manner, which can be challenging by itself. It is furthermore unclear, under which circumstances which accuracy of delay interpolation is sufficient. Listening experiments have to be conducted to acquire perceptually motivated guidelines.

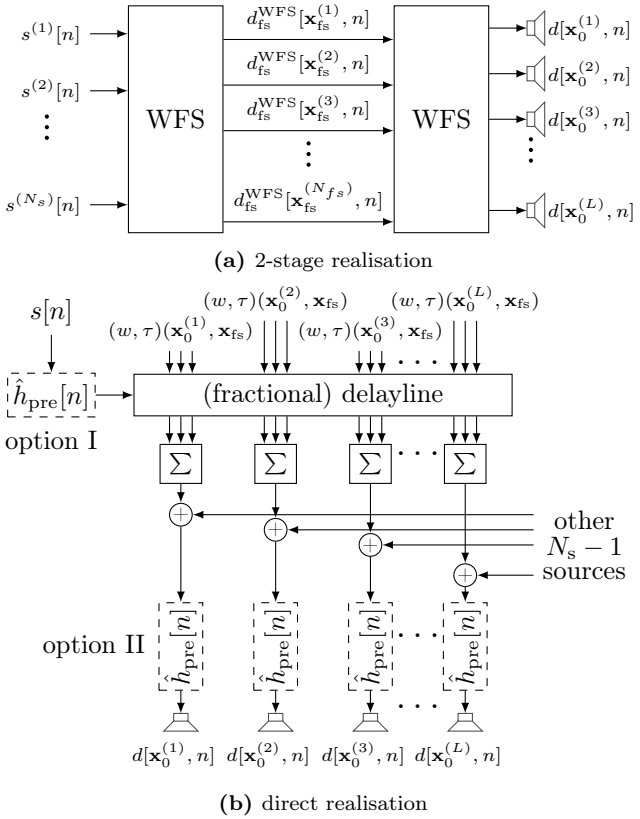

(a) 2-stage realisation

(b) direct realisation

Figure 4: Block diagrams showing the two time-domain realisations of Local Wave Field Synthesis.

References

[1] A. J. Berkhout. "A Holographic Approach to Acoustic Control". In: *J. Aud. Eng. Soc.* 36.12 (1988), pp. 977–995.

[2] J. Daniel. "Spatial Sound Encoding Including Near Field Effect: Introducing Distance Coding Filters and a Viable, New Ambisonic Format". In: *Proc. of 23rd Intl. Aud. Eng. Soc. Conf. on Signal Processing in Audio Recording and Reproduction*. 2003.

[3] E. Corteel, C. Kuhn-Rahloff, and R. Pellegrini. "Wave Field Synthesis Rendering with Increased Aliasing Frequency". In: *Proc. of 124th Aud. Eng. Soc. Conv.* Amsterdam, The Netherlands, 2008.

[4] J. Hannemann and K. D. Donohue. "Virtual Sound Source Rendering Using a Multipole-Expansion and Method-of-Moments Approach". In: *J. Aud. Eng. Soc.* 56.6 (2008), pp. 473–481.

[5] Y. J. Wu and T. D. Abhayapala. "Spatial multizone soundfield reproduction". In: *2009 IEEE International Conference on Acoustics, Speech and Signal Processing*. 2009, pp. 93–96. DOI: 10.1109/ICASSP.2009.4959528.

[6] S. Spors, K. Helwani, and J. Ahrens. "Local sound field synthesis by virtual acoustic scattering and time-reversal". In: *Proc. of 131st Aud. Eng. Soc. Conv.* Audio Engineering Society (AES). New York, USA, 2011.

[7] N. Hahn, F. Winter, and S. Spors. "Local Wave Field Synthesis by Spatial Band-Limitation in the Circular/Spherical Harmonics Domain". In: *Proc. of 140th Aud. Eng. Soc. Conv.* Paris, France, 2016, pp. 1–12.

[8] S. Spors and J. Ahrens. "Local Sound Field Synthesis by Virtual Secondary Sources". In: *Proc. of 40th Intl. Aud. Eng. Soc. Conf. on Spatial Audio*. Tokyo, Japan, 2010.

[9] E. N. G. Verheijen. "Sound Reproduction by Wave Field Synthesis". PhD thesis. Delft University of Technology, 1997.

[10] E. G. Williams. *Fourier Acoustics: Sound Radiation and Nearfield Acoustical Holography*. London: Academic Press, 1999.

[11] S. Spors, R. Rabenstein, and J. Ahrens. "The theory of Wave Field Synthesis revisited". In: *Proc. of 124th Aud. Eng. Soc. Conv.* Amsterdam, The Netherlands, 2008.

[12] F. Schultz. "Sound Field Synthesis for Line Source Array Applications in Large-Scale Sound Reinforcement". PhD thesis. University of Rostock, 2016.

[13] A. Franck. "Efficient Algorithms for Arbitrary Sample Rate Conversion with Application to Wave Field Synthesis". PhD thesis. Technische Universität Ilmenau, 2011.

[14] J Ahrens, M Geier, and S Spors. "Perceptual Assessment of Delay Accuracy and Loudspeaker Misplacement in Wave Field Synthesis". In: *Proc. of 128th Aud. Eng. Soc. Conv.* London, UK, 2010.

[15] A. Franck et al. "Reproduction of Moving Sound Sources by Wave Field Synthesis: An Analysis of Artifacts". In: *Proc. of 32nd Intl. Aud. Eng. Soc. Conf. on DSP For Loudspeakers*. Hilleroed, Danmark, 2007.

[16] M. Geier and S. Spors. "Spatial Audio with the SoundScape Renderer". In: *27th Tonmeistertagung – VDT International Convention*. Cologne, Germany, 2012.